

Supporting Information

Water-induced Dual Ultrahigh Mobilities Over 400 cm²/Vs in 2D MoS₂ Transistor for Ultralow-voltage Operation and Photoelectric Synapse Perception

Dingdong Xie, Liubo Wei, Ziqing Wei, Jun He*, and Jie Jiang*

Hunan Key Laboratory of Nanophotonics and Devices, School of Physics and Electronics, Central South University, 932 South Lushan Road, Changsha, Hunan 410083, P. R. China

E-mail: junhe@csu.edu.cn;

jiangjie@csu.edu.cn

Supplementary Note 1. The spike number-dependent EPSCs

As shown in Fig. S6, the spike number-dependent EPSC responses can be studied in the proposed water-induced MoS₂ synapse. The presynaptic spike is fixed at (V_b : -0.2 V, V_{spike} : 0.4 V, duration time: 20 ms). From this figure, it is clearly seen that the peak amplitude of EPSC increases from 0.49 μA to 0.54 μA with the stimulus number ranging from 1 to 20. The possible reason is that the superimposition of spike stimuli within the relaxation time leads to a corresponding increase in the number of channel electrons, ultimately leading to a larger EPSC response.^{1,2} At the same time, the T_m can be extracted from these spike number-dependent EPSCs, as shown in the inset of Fig. S6. It is obvious that the T_m increases almost linearly within a small stimulus number below 5, while it will get saturated when the stimulus number is above 10. Moreover, the interesting phenomenon can be well fitted by using the exponential model as the following equation:¹

$$T_m = f(N) = A \cdot \exp\left(\frac{-N}{\tau_N}\right) + T_\infty \quad (\text{S1})$$

where T_∞ and A represent the ultimate value of T_m and the original facilitation magnitude of memory process, respectively. The τ_N represents the characteristic constant of stimulus number. By fitting with Eq. S1, A and T_∞ are obtained as -0.37 s and 0.61 s, respectively. Notably, τ_N can be extracted as 3.79, revealing that our device has fast memory ability when the stimulus number is less than τ_N .^{2,3} Such results indicate that the artificial MoS₂ synapse with adjustable memory behavior is of great significance to the future development of bionic storage systems.¹⁻³

Supplementary Note 2. The spike number-dependent IPSCs

Fig. S7 shows the spike number-dependent IPSC responses in our water-induced MoS₂ synapse. The presynaptic spike is fixed at (V_b : 0.4 V, V_{spike} : -0.2 V, duration time: 20 ms). It is obvious that the IPSC amplitude increases with the number of presynaptic spike. This is because that the MoS₂ device has turn-off properties under the negative stimulus.⁴ Moreover, repeated negative spike stimuli would lead to a greater reduction in the number of channel electrons, resulting in a lower IPSC response.^{5,6} Meanwhile, the spike number-dependent Δ IPSC can be also extracted as shown in the inset of Fig. S7. From this figure, the absolute value of Δ IPSC increases from to 0.33 μ A to 0.37 μ A with the stimulus number ranging from 1 to 20. The realization of spike number-dependent IPSC behavior through the proposed device is very beneficial for neuromorphic computing in biological systems.

Supplementary Note 3. The decoding of Morse-coded “HELP”

The Morse-coded message of “HELP” is decoded by the proposed water-induced MoS₂ synapse as well, as shown in Fig. S9a,b. From these figures, it is clearly seen that the PSC amplitude increases significantly when V_{DS} changes from 0.01 V to 0.2 V due to the FETs theory.⁴ Meanwhile, the SNR of Morse-coded “HELP” can be extracted as shown in Fig. S9c,d. It is obvious that the absolute value of SNR increases linearly with the increase of V_{DS} . Interestingly, the relationship between SNR and V_{DS} can be also well fitted by a linear equation by Eq. 5 of main text. The fitting results of S_k and S_0 can be obtained as 306.12 V⁻¹ and 34.75 for EPSC-induced “SHELP”. Meanwhile, the Fig. S9d can be also fitted using the equation, and the S_k and S_0 are found to be 23.23 V⁻¹ and 4.99, respectively. Such fitting results indicate that the SNR caused by EPSC and IPSC are complementary processes that can be closely coordinated, which is particularly useful for being able to perform noise removal and unsupervised feature learning tasks simultaneously.⁷

Supplementary Figures

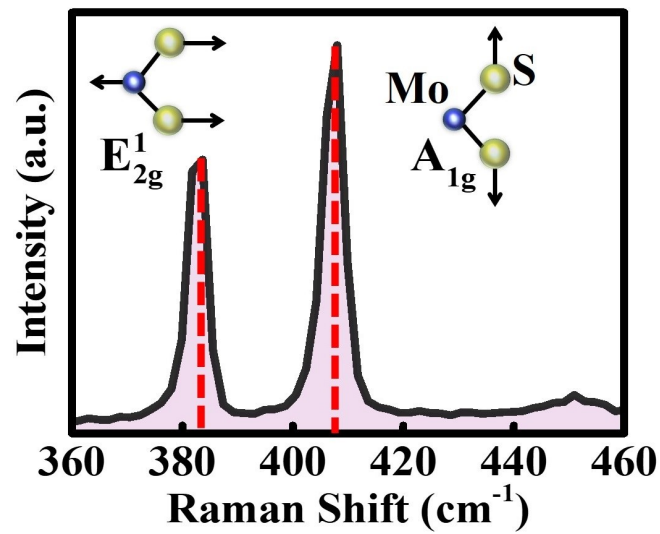


Fig. S1. Raman-spectra of MoS₂ flake. Inset: schematic diagram of in-plane E_{2g}¹ mode and out-of-plane A_{1g} mode in MoS₂. The E_{2g}¹ mode refers the in-plane opposing motions of molybdenum and sulfur atoms, while the A_{1g} mode involves the out-of-plane relative motions of sulfur atoms.

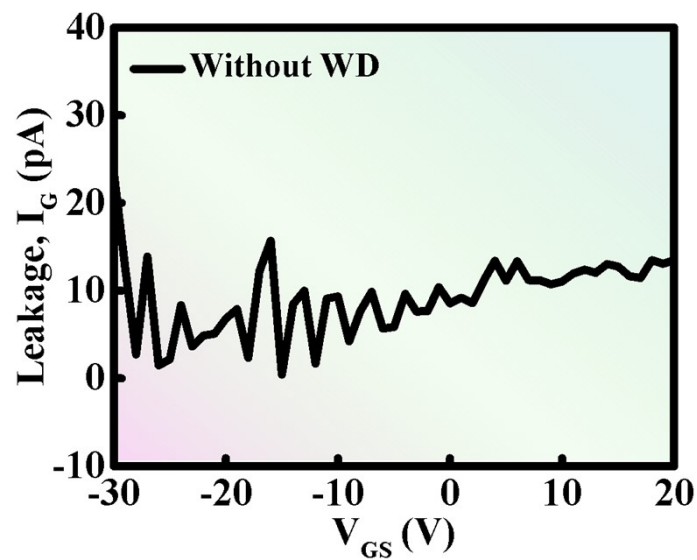


Fig. S2. The leakage current of the MoS₂ FET without WD for the voltage sweeping from -30 V to 20 V.

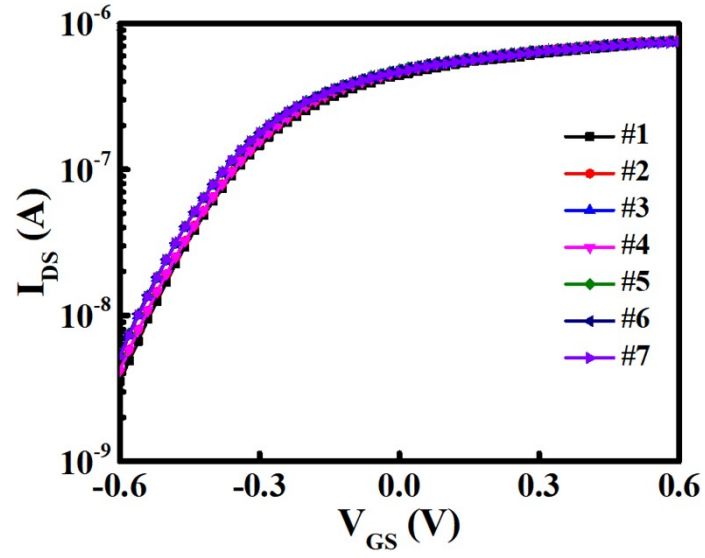


Fig. S3. Transfer curve of the water-induced MoS₂ FET under the fixed bias of $V_{DS}=0.1$ V for seven successive measurements.

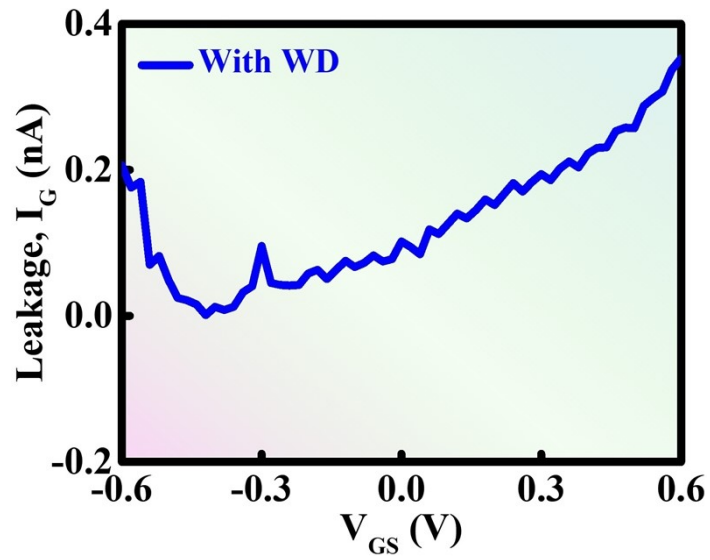


Fig. S4. The leakage current of the water molecules for the voltage sweeping from -0.6 V to 0.6V.

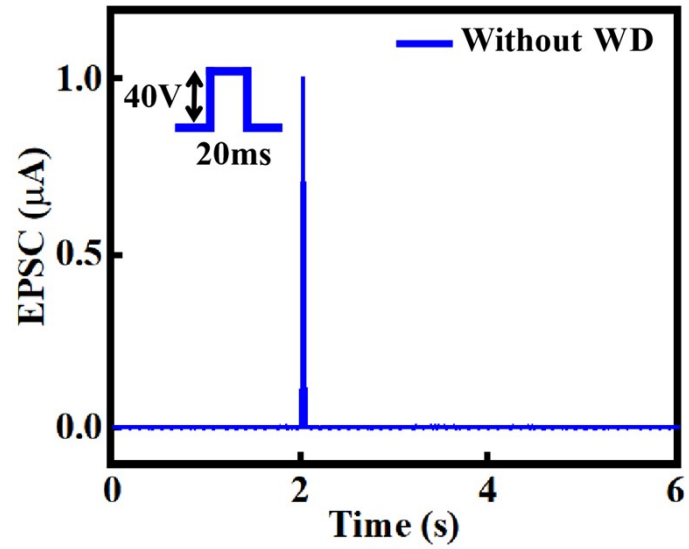


Fig. S5. EPSC induced by presynaptic spike (V_b : -20 V, V_{spike} : 20 V, duration time: 20 ms) without WD.

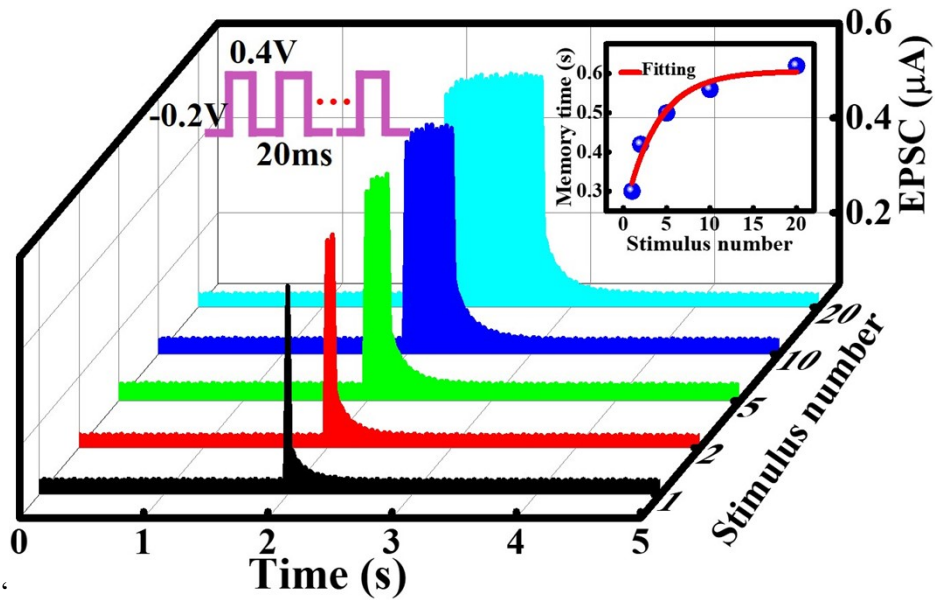


Fig. S6. EPSCs induced by presynaptic spikes (V_b : -0.2 V, V_{spike} : 0.4 V, duration time: 20 ms) with different stimulus number. Inset: memory time as a function of stimulus number.

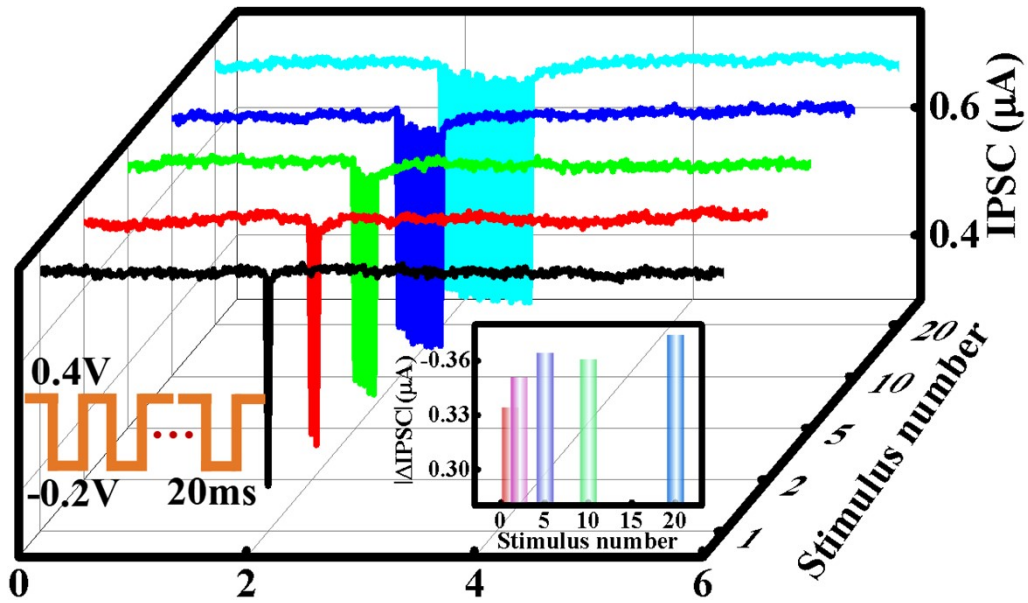


Fig. S7. IPSCs induced by presynaptic spikes (V_b : 0.4 V, V_{spike} : -0.2 V, duration time: 20 ms) with different stimulus number. Inset: ΔIPSC as a function of stimulus number.

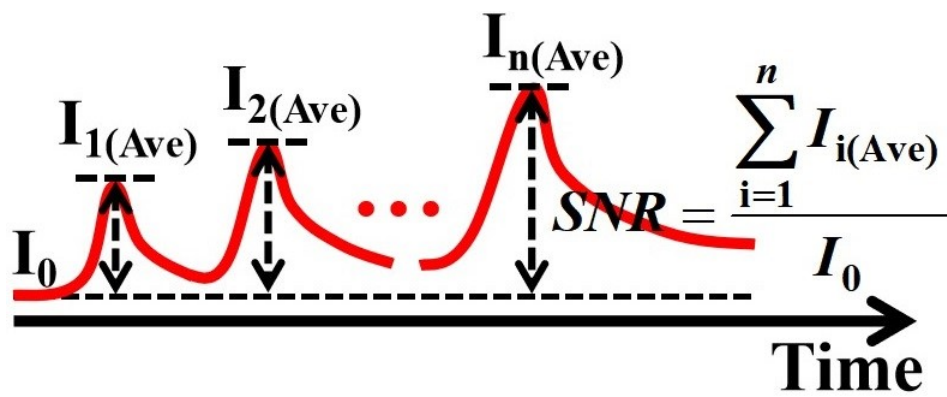


Fig. S8. The schematic diagram of the equation definition of SNR.

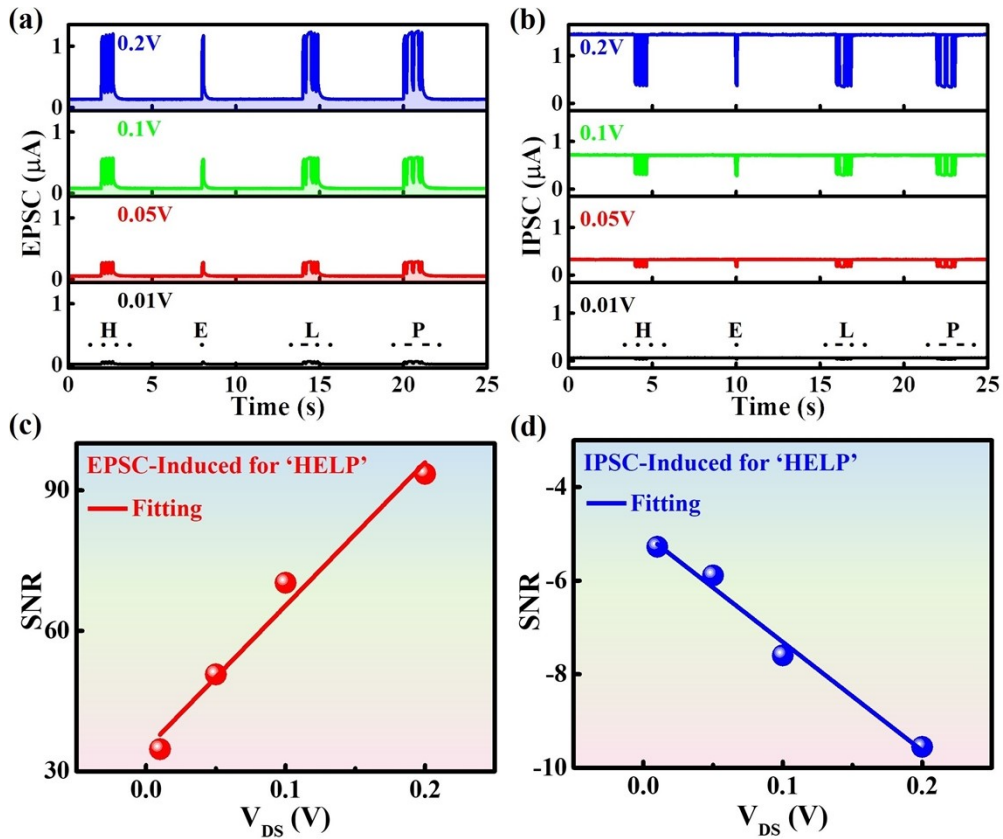


Fig. S9. (a) Spike duration-dependent EPSCs under different V_{DS} expressing the International Morse code of “HELP”. (b) Spike duration-dependent IPSCs under different V_{DS} expressing the International Morse code of “HELP”. (c) The SNR caused by EPSC as a function of V_{DS} . (d) The SNR caused by IPSC as a function of V_{DS} .

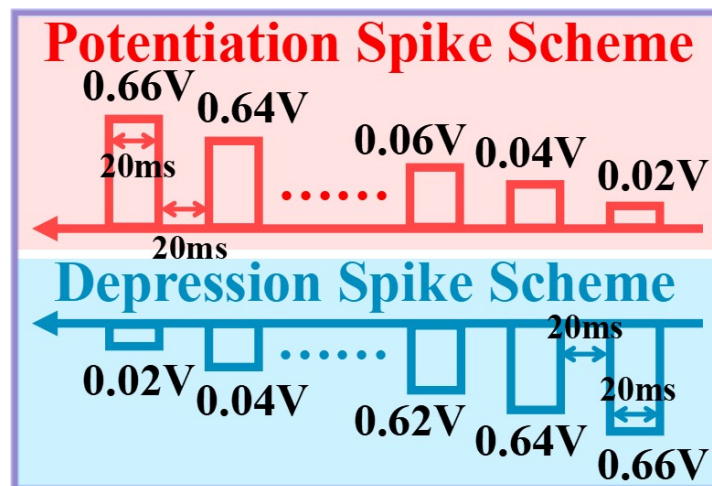


Fig. S10. Spike schemes for potentiation and depression applied to the bottom-gate.

Supplementary References

- 1 T. Ahmed, S. Kuriakose, E. L. H. Mayes, R. Ramanathan, V. Bansal, M. Bhaskaran, S. Sriram, S. Walia, *Small*, 2019, **15**, 1900966.
- 2 Y. Zhao, B. Liu, J. Yang, J. He, J. Jiang, *Chin. Phys. Lett.*, 2020, **37**, 088501.
- 3 S.-T. Lee, S. Y. Woo, J.-H. Lee, *IEEE Access*, 2020, **8**, 153334-153340.
- 4 B. Radisavljevic, A. Radenovic, J. Brivio, V. Giacometti, A. Kis, *Nat. Nanotechnol.*, 2011, **6**, 147-150.
- 5 D. Xie, W. Hu, J. Jiang, *Org. Electron.*, 2018, **63**, 120-128.
- 6 J. Jiang, Y. Zhang, A. Wang, J. Duan, H. Ji, J. Pang, Y. Sang, X. Feng, H. Liu, L. Han, *ACS Appl. Electron. Mater.*, 2020, **2**, 2132-2140.
- 7 S. Afshar, L. George, C. S. Thakur, J. Tapson, A. van Schaik, P. de Chazal, T. J. Hamilton, *IEEE T. Biomed. Circ. S.*, 2015, **9**, 188-196.